ARTICLES

A Study on Hydrogen-Bonded Network Structure of Polybenzoxazines†

Ho-Dong Kim and Hatsuo Ishida*

NSF Center for Molecular and Microstructure of Composites (CMMC), Department of Macromolecular Science and Engineering, Case Western Reserve University, Cleveland, Ohio 44106

Received: February 15, 2001

The hydrogen-bonded network structure for polybenzoxazines is investigated by Fourier Transform Infrared Spectroscopy (FT-IR) with model dimer systems. Comparing the FT-IR spectra of the polybenzoxazines and model dimers, it is shown that the simpler structures of asymmetric dimers well simulate the hydrogen-bonded network structure between polymer chains while the structures of symmetric dimers reflect the hydrogen bonding scheme related to the end-groups of polymer chains. It is confirmed that the amine functional group in the Mannich bridge is greatly responsible for the distribution of hydrogen bonding species. Bisphenol A/methylamine-based polymer (BA-m) mainly consists of −OH···N intramolecular hydrogen bonding while bisphenol A/aniline-based polymer (BA-a) has a large amount of intermolecular hydrogen bonding and relatively weak hydrogen bonding groups in the polymer network structure. The possible network structure, in the sense of hydrogen bonding, for BA-m and BA-a polymers is proposed and a generalized explanation for the structure−property relationships in polybenzoxazines is also discussed.

Introduction

Recently, polybenzoxazines having a number of unique properties have been actively studied. This class of polymers has many advantages such as excellent mechanical properties,[1,2] high char yield,[2] near zero volumetric shrinkage/expansion upon polymerization,[3] low water absorption despite the large amount of hydroxyl groups in the backbone structure, excellent resistance to chemicals[4] and UV light,[5] and high T_g.[6] For several years, these properties have been extensively studied to achieve a good molecular understanding of the polymer, as well as to meet the industrial interests.

According to Ishida and Allen,[1] it has been determined that the network structure of polybenzoxazine is supported by the interaction of polymer chains due to strong hydrogen bonding, as well as chemical cross-linking. Therefore, taking into account the low cross-linking density in polybenzoxazines, the role of hydrogen bonding in the polymer system is of great importance in interpreting structure−property relationships. Despite the similar chemical structure of BA-m polymer and BA-a polymer, they have different FT-IR spectra in the region of the hydroxyl stretching frequencies as shown in Figure 1. This has been simply explained by the fact that the strength of hydrogen bonding is dependent on the electronegativity of the side group that is attached to the nitrogen atom (Scheme 1). That is, the electron cloud density around the nitrogen atom attached to the benzene ring is lower than that of the BA-m polymer because the electrons on the nitrogen atom in BA-a polymer are more delocalized.

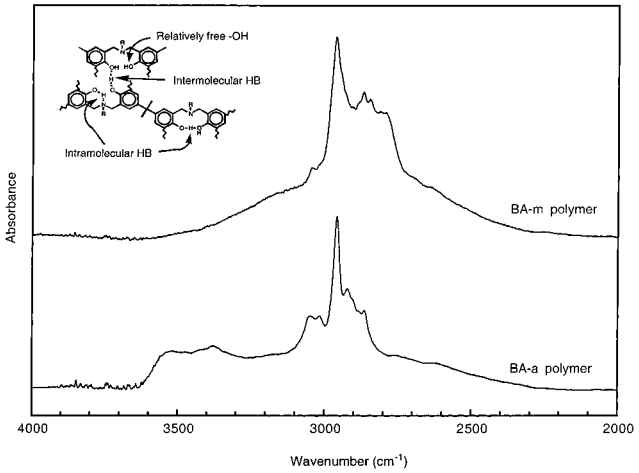

Figure 1. Comparison of the FTIR spectra for BA-m and BA-a polybenzoxazines in the region of hydroxyl stretching frequency.

This network structure in polybenzoxazines, which is supported by hydrogen bonding, might be a possible and important contribution to forming a rigid network structure. However, despite the importance of hydrogen bonding in polybenzoxazines, only a few papers[1,7,8] have been reported because it is difficult to analyze the structure of polybenzoxazines due to the instrumental limitations for thermoset resins. In addition, since the polybenzoxazine structure can form several different hydrogen bonding species between hydroxyl groups or between hydroxyl group and tertiary nitrogen atom, it has been even more difficult to study the structure. Furthermore, although it was postulated in previous papers that the physical properties of polybenzoxazines including chemical and UV stability may

† Part of the special issue "Mitsuo Tasumi Festschrift".
* Author to whom correspondence should be addressed.

10.1021/jp010606p CCC: $22.00
Published on Web 06/07/2001

SCHEME 1: Difference of Electronegativity around the Nitrogen Atom in Mannich Bridge (A) Methylamine-Based Structure, and (B) Aniline-Based Structure

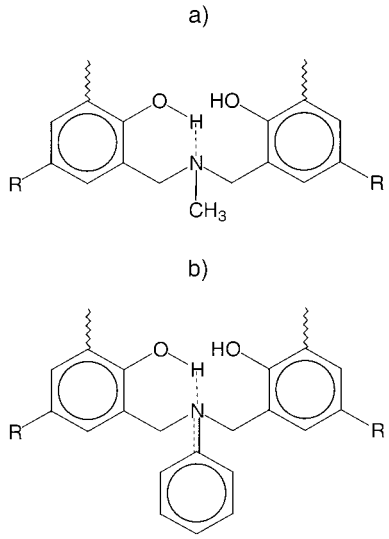

also be related to the nature of the amines,[4,5] the distribution of hydrogen bonding species in polybenzoxazine has not been evaluated. In addition, the reason two typical polybenzoxazines have significantly different properties is not clear.

In this paper, we will, therefore, investigate the hydrogen-bonded network structure of polybenzoxazines using well-designed polybenzoxazine model dimer molecules. Additionally, this paper intends to establish the generalized explanation between the physical properties of polybenzoxazines and the network structure.

Experimental Section

All chemicals were used as received. Bisphenol A (97%), *p*-formaldehyde (95%), aniline (99%), methylamine (40% in water), 2,4-dimethylphenol (98%), benzylbromide (98%), salicylaldehyde (98%), *N*-methylbenzylamine (97%), and *N*-phenylbenzylamine (99%) were obtained from Aldrich Chemical Co. Formaldehyde (37% in water) was purchased from Fisher Scientific.

Synthesis of Benzoxazine Monomers and Polymers. Two typical bifunctional benzoxazine monomers were synthesized and purified according to the procedure of Ning and Ishida[9] or Ishida.[10] One was 2,2-bis(3,4-dihydro-3-methyl-2H-1,3-benzoxazine)propane (abbreviated as BA-m) based on methylamine and the other was 2,2-bis(3,4-dihydro-3-phenyl-2H-1,3-benzoxazine)propane (abbreviated as BA-a) based on aniline. The purity of the compounds was determined using 200 MHz proton nuclear magnetic resonance (^{1}H NMR) spectra. These benzoxazine monomers were polymerized without added initiator or catalyst according to the method which was shown in the previous paper.[4] R in the structure denotes the substituent of the primary amine (Scheme 2).

Synthesis of a Methylamine-Based Polybenzoxazine Model Dimer. *N*,*N*-Bis(3,5-dimethyl-2-hydroxybenzyl)methylamine (Scheme 3a) was synthesized according to a previous study using 2,4-dimethylphenol, formaldehyde, and methylamine.[11] White, irregular crystals were obtained by recrystallization from ethyl ether for the methylamine-based dimer. White crystal. ^{1}H NMR (200 MHz, $CDCl_3$, 298 K) δ: 2.22 (12H, Ar$-CH_3$), δ: 2.24 (3H, N$-CH_3$), 3.66 (4H, Ar$-CH_2-$N), and 6.73, 6.89 (4H, Ar$-$H). ^{13}C NMR (50.1 MHz, $CDCl_3$, 298 K) δ: 15.74, 20.41 (4C, Ar$-$C), 41.06 (1C, N$-CH_3$), 59.25 (2C, Ar$-$C$-$N), and 121.80$-$152.00 (12C, Ar). Anal. Found: C, 76.40; H, 8.54; N, 4.60. Calcd. For $C_{19}H_{25}NO_2$: C, 76.22; H, 8.42; N, 4.68.

SCHEME 2: Bis-phenol A-Based Benzoxazine Monomer

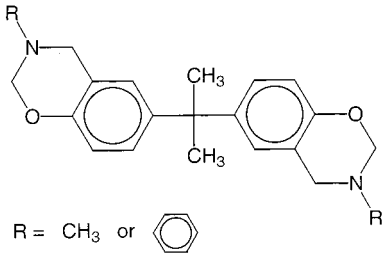

Synthesis of an Aniline-Based Polybenzoxazine Model Dimer. *N*,*N*-Bis(3,5-dimethyl-2-hydroxybenzyl)aniline (Scheme 3d) was also synthesized by the method described in the previous paper.[11] The product was recrystallized from hexane until white crystals were obtained and subsequently purified by column separation. White needlelike crystal. ^{1}H NMR (200 MHz, $CDCl_3$, 298 K) δ: 2.16, 2.17 (12H, Ar$-CH_3$), 4.26 (4H, Ar$-CH_2-$N), 6.65, 6.82 (4H, Ar$-$H), and 7.00$-$7.31 (5H, Ar$-$H). ^{13}C NMR (50.1 MHz, $CDCl_3$, 298 K) δ: 15.84, 20.48 (4C, Ar$-$C), 55.68 (2C, Ar$-$C$-$N), and 121.60$-$151.70 (18C, Ar). Anal. Found: C, 79.89; H, 7.69; N, 3.91. Calcd. For $C_{24}H_{27}NO_2$: C, 79.74; H, 7.53; N, 3.87.

Synthesis of an Asymmetric Methylamine-Based Model Dimer. *N*-Benzyl-*N*-(3,5-dimethyl-2-hydroxylbenzyl)methylamine (Scheme 3b) was synthesized using 2,4-dimethylphenol, *p*-formaldehyde, and *N*-methylbenzylamine as follows. A solution of 2,4-dimethylphenol (0.05 mol), *p*-formaldehyde (0.05 mol), and *N*-methylbenzylamine (0.05 mol) was azeotropically distilled in *n*-hexane until 0.9 mL of water had been collected. The hexane solution was washed several times with distilled water, and dried over sodium sulfate. The residual products were purified by column chromatography on silica gel using hexane/tetrahydrofuran (10:1) as the eluent. Pale yellow liquid. ^{1}H NMR (200 MHz, $CDCl_3$, 298 K) δ: 2.20, 2.21 (9H, $-CH_3$), 3.58, 3.69 (4H, Ar$-CH_2-$N), 6.65, 6.86 (2H, Ar$-$H), and 7.24$-$7.38 (5H, Ar$-$H). ^{13}C NMR (50.1 MHz, $CDCl_3$, 298 K) δ: 15.64, 20.38 (2C, Ar$-$C), 41.05 (1C, N$-$C), 61.03, 61.50 (2C, Ar$-$C$-$N), and 120.73$-$153.47 (12C, Ar). Anal. Found: C, 80.07; H, 8.15; N, 5.56. Calcd. For $C_{17}H_{21}NO$: C, 79.96; H, 8.29; N, 5.49.

Synthesis of an Asymmetric Aniline-Based Model Dimer. *N*-Benzyl-*N*-(3,5-dimethyl-2-hydroxylbenzyl)aniline (Scheme 3e) was synthesized using 2,4-dimethylphenol, *p*-formaldehyde, and *N*-phenylbenzylamine as follows. A solution of 2,4-dimethylphenol (0.05 mol), *p*-formaldehyde (0.05 mol), and *N*-phenylbenzylamine (0.05 mol) was reacted at 105 °C for 1 h. The products were then dissolved in chloroform, washed several times with distilled water, and dried over sodium sulfate. The residual products were purified by column chromatography on silica gel using hexane/ethyl acetate (5:1) as the eluent. Pale yellow liquid. ^{1}H NMR (200 MHz, $CDCl_3$, 298 K) δ: 2.20, 2.22 (6H, Ar$-CH_3$), 4.27, 4.31 (4H, Ar$-CH_2-$N), 6.69, 6.86 (2H, Ar$-$H), and 6.68$-$7.35 (10H, Ar$-$H). ^{13}C NMR (50.1 MHz, $CDCl_3$, 298 K) δ: 15.62, 20.48 (2C, Ar$-$C), 55.19, 57.68 (2C, Ar$-$C$-$N), and 112.81 $\sim$ 152.84 (18C, Ar). Anal. Found: C, 83.49; H, 7.12; N, 4.63. Calcd. For $C_{22}H_{23}NO$: C, 83.24; H, 7.30; N, 4.41.

Synthesis of Dibenzylmethylamine. *N*,*N*-Dibenzylmethylamine (Scheme 3c) was synthesized using benzylbromide and

SCHEME 3: Polybenzoxazine Model Dimers. (A) Methyl-dimer, (B) Asymmetric Methyl-dimer, (C) Benzylic Methyl-dimer, (D) Aniline-dimer, (E) Asymmetric Aniline-dimer, and (F) Benzylic Aniline-dimer

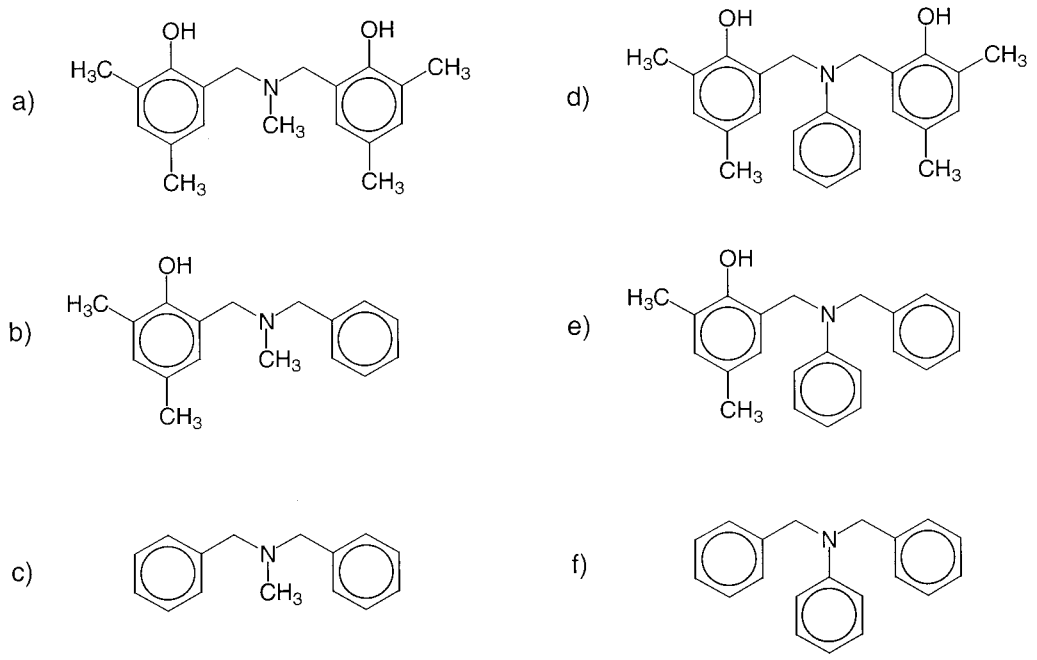

methylamine as follows.[12] A stoichiometric amount of reactants (benzylbromide: methylamine = 2:1) were reacted in ethyl ether at room temperature for 10 min and the viscous product dissolved in ethyl ether. The ether solution was washed several times with distilled water, and dried over sodium sulfate. The residual products were purified by column chromatography on silica gel using hexane/methylene chloride (3:2) as eluent. Pale yellow liquid. ^{1}H NMR (200 MHz, $CDCl_3$, 298 K) δ: 2.17 (3H, $-CH_3$), 3.51 (4H, Ar$-CH_2-$N), and 7.19−7.38 (10H, Ar−H). ^{13}C NMR (50.1 MHz, $CDCl_3$, 298 K) δ: 42.24 (1C, N−C), 61.85 (2C, Ar−C−N), and 126.87−139.31 (12C, Ar). Anal. Found: C, 85.06; H, 7.98; N, 6.44. Calcd. For $C_{15}H_{17}N$: C, 85.26; H, 8.11; N, 6.63.

Synthesis of Dibenzylaniline. *N*,*N*-Dibenzylaniline (Scheme 3f) was synthesized using benzylbromide and aniline as follows. A solution of benzylbromide (0.04 mol) and aniline (0.06 mol) in chloroform was reacted at room temperature with vigorous stirring for 1 h. An excess amount of aniline was used as an acid-trap as well as reactant. The mixture was then dissolved in chloroform and the organic layer was separated, dried over sodium sulfate, and evaporated. The residual products were purified by column chromatography on silica gel using hexane/methylene chloride (5:1) as eluent. Pale yellow liquid. ^{1}H NMR (200 MHz, $CDCl_3$, 298 K) 4.65 (4H, Ar$-CH_2-$N), and 6.65−7.35 (15H, Ar−H). ^{13}C NMR (50.1 MHz, $CDCl_3$, 298 K) δ: 54.15 (2C, Ar−C−N), and 112.39−138.54 (18C, Ar). Anal. Found: C, 87.69; H, 7.19; N, 5.02. Calcd. For $C_{20}H_{19}N$: C, 87.87; H, 7.01; N, 5.12.

The purity of the dimers was examined using a Varian XL200 nuclear magnetic resonance spectrometer (^{1}H NMR and ^{13}C NMR) and a Hewlett-Packard 6890 Gas Chromatograph equipped with a 5973 Mass Selective Detector (GC-MS). For simplicity, *N*,*N*-bis(3,5-dimethyl-2-hydroxybenzyl)methylamine, *N*,*N*-bis(3,5-dimethyl-2-hydroxybenzyl)aniline, *N*,*N*-dibenzylmethylamine, *N*,*N*-dibenzylaniline, *N*-benzyl-*N*-(2-hydroxylbenzyl)methylamine, and *N*-benzyl-*N*-(3,5-dimethyl-2-hydroxylbenzyl) will be referred to as Methyl-dimer, Aniline-dimer, asymmetric Methyl-dimer, asymmetric Aniline-dimer, benzylic Methyl-dimer, and benzylic Aniline-dimer in this paper, respectively.

Fourier transform infrared (FT-IR) spectra were obtained on a Bomem Michelson MB110 FT-IR spectrophotometer which was equipped with a liquid nitrogen cooled, mercury cadmium telluride (MCT) detector with a specific detectivity, D^*, of 1×10^{10} cm Hz$^{1/2}$ W^{-1}. Coaddition of 128 scans was recorded at a resolution of 4 cm^{-1} after 20 min purge with dry nitrogen. FT-IR spectra of the BA-m and BA-a polymers were taken from the thin films cured on potassium bromide (KBr) plates, using the same procedure in a previous paper.[4] The crystalline dimer spectra for Methyl-dimer and Aniline-dimer were taken as a thin powder layer between two KBr plates. The spectra for the benzylic Methyl-dimer, benzylic Aniline-dimer, asymmetric Methyl-dimer, and asymmetric Aniline-dimer in pure liquid phase were collected from a thin layer between two KBr plates. The KBr pellet technique was not used to avoid water from interfering with the OH stretching region of interest. The solution spectra for the dimers in CCl_4 were obtained in a barium fluoride liquid cell with a 0.5 mm thickness for 10 mM and 50 mM concentrations and with a 5 mm thickness for 1 mM concentration. The spectrum of the liquid cell with spectrophotometric grade carbon tetrachloride (CCl_4) was subtracted from the solution spectra.

Heavily overlapped bands in the hydroxyl stretching region of FT-IR spectrum from 2000 to 4000 cm^{-1} were curve-resolved using a mixed Lorentzian−Gaussian function in GRAMS software. It was calculated until the least-squares curve-fitting converged.

Results

Symmetric Dimers. To simulate the distribution of hydrogen-bonded species in polybenzoxazines, the FT-IR spectra for several benzoxazine model dimers were investigated. Since benzylic dimers do not have hydroxyl stretching bands, they show flat baselines in the hydrogen-bonded hydroxyl stretching regions as shown in Figures 2c and 3c. Since the chemical structures of the symmetric and asymmetric dimers are similar to benzylic dimmers, except for the hydroxyl groups, the hydroxyl stretching regions of FT-IR spectra for the symmetric

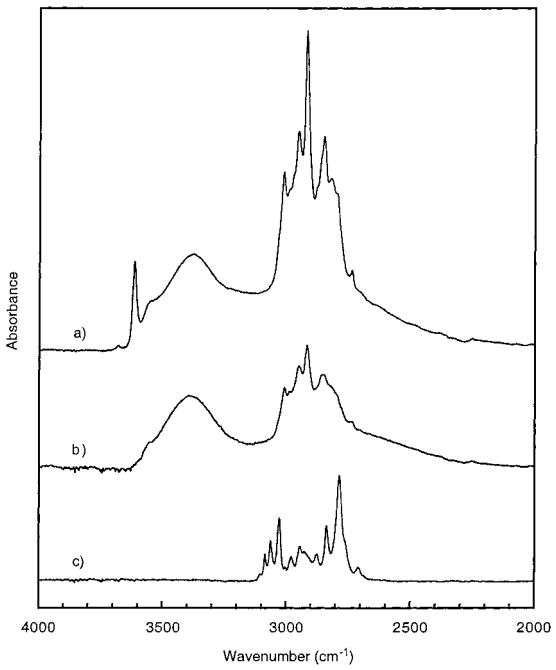

Figure 2. FT-IR spectra for (a) Methyl-dimer in solution state in CCl_4 (50 mM), (b) Methyl-dimer in crystal state, and (c) benzylic Methyl-dimer in liquid phase.

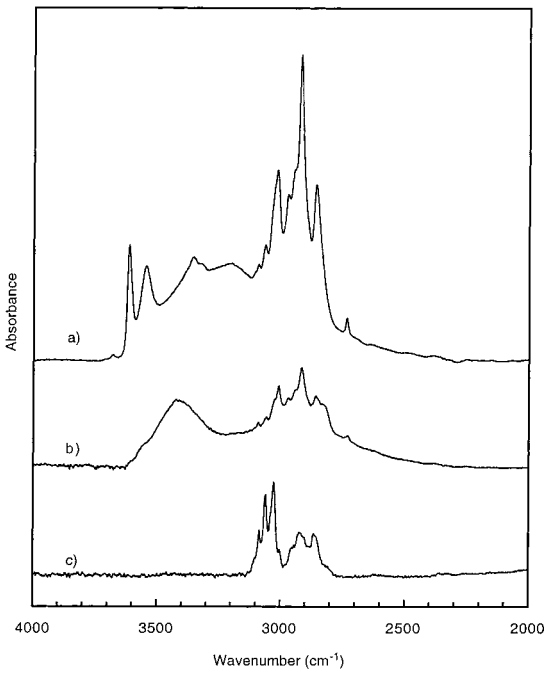

Figure 3. FT-IR spectra for (a) Aniline-dimer in solution state in CCl_4 (50 mM), (b) Aniline-dimer in crystal state, and (c) benzylic Aniline-dimer in liquid phase.

and asymmetric dimers will reflect the distribution of hydrogen bonding in the dimers. In the study of hydrogen bonding for a benzoxazine model dimer using methylamine by Dunkers,[7] it was shown that it is possible to form several kinds of hydrogen-bonded species, such as −OH···O intermolecular hydrogen bonding, −OH···O intramolecular hydrogen bonding, and −OH···N intramolecular hydrogen bonding. The band centered at 3400 cm^{-1} in Figure 2b shows the existence of −OH···O intermolecular hydrogen bonding, and the broad band between 2500 and 3300 cm^{-1} might be designated for −OH···O intramolecular hydrogen bonding and/or −OH···N intramolecular hydrogen bonding. Consequently, this result has been used to explain the network structure and good physical properties of polybenzoxazines reported in many papers.

However, despite the understanding that the hydrogen bonding in the Mannich bridge is strongly affected by the basicity of amine functional group which is attached to the nitrogen atom, the actual difference between the Methyl-dimer and Aniline-dimer was overlooked with regard to hydrogen bonding. The analysis of the aniline-based model system is essential in order to interpret the more realistic hydrogen bonding structure in the BA-a polymer. Therefore, the model Aniline-dimer for the BA-a polymer is synthesized and the FT-IR spectrum is investigated.

Surprisingly, despite the large difference in basicity in the corresponding amines, the FT-IR spectra for the two model dimer crystals show very similar features (Figures 2b and 3b). Taking into account the fact that the nature of hydrogen bonding in Mannich bases is closely related to the acidity of the parent phenol or basicity of the amine functional group,[13] it was expected that the distribution of hydrogen bonding species in Aniline-dimer should be different. However, from the similar spectra for both model dimer crystals, it seems that the basicity of the amine functional group has little influence on the hydrogen bonding structure in the crystal lattice. Since the molecules in crystal form have an order in a certain lattice cell and are closely arranged to each other, the hydrogen bonding structure is highly affected by the physical packing of molecules. Therefore, it is possible that there is no significant difference in the spectrum of the crystal state for both model dimers if both model dimers have similar crystal structures.

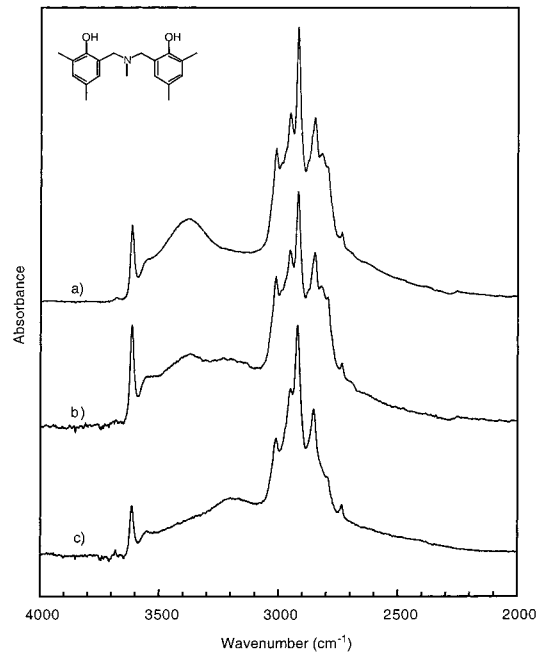

Figure 4. FT-IR spectra for Methyl-dimer in CCl_4 solution; (a) 50 mM, (b) 10 mM, and (c) 1 mM concentration.

In solution, however, the dimer molecules can freely change their relative positions and have wide spaces between them, thus allowing the intermolecular and intramolecular hydrogen bonding to be distinguished by examining CCl_4 solution spectra at various concentrations. Figure 4 shows the FT-IR spectra of Methyl-dimer at various concentrations in CCl_4. In Figure 4a, the spectrum for a concentration of 50 mM shows significant

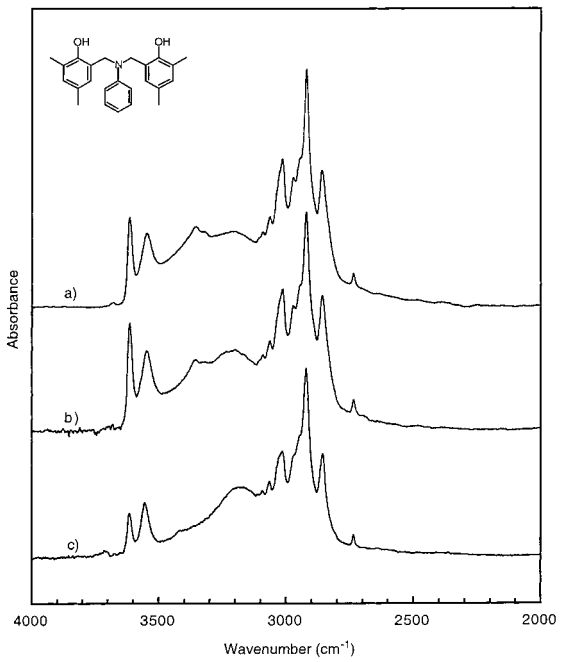

Figure 5. FT-IR spectra for Aniline-dimer in CCl_4 solution; (a) 50 mM, (b) 10 mM, and (c) 1 mM concentration.

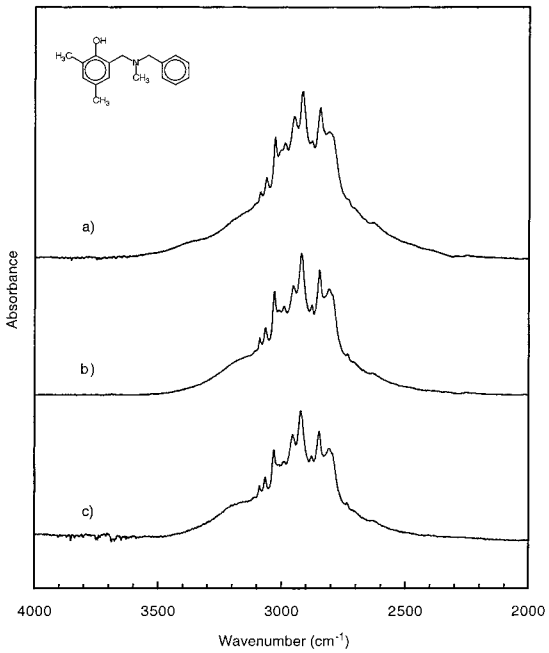

Figure 6. FT-IR spectra for asymmetric Methyl-dimer (a) in liquid phase, (b) in solution state in CCl_4 (50 mM), and (c) in solution state in CCl_4 (1 mM).

intermolecular hydrogen bonding as demonstrated by the strong band at 3401 cm^{-1} as well as free hydroxyl groups (3615 cm^{-1}) due to the dilution of the dimer molecules. This assignment for intermolecular hydrogen bonding is confirmed by the fact that the intensity of this band at 3401 cm^{-1} is systematically decreased by the decrease in concentration. Figure 4c displays the spectrum of 1 mM of Methyl-dimer in CCl_4. If intramolecular hydrogen bonding is not present, all the hydroxyl groups are expected to be free at this concentration as has been shown in studies on hydrogen bonding in phenolic dimers.[14,15] Obviously, two evident bands for the free hydroxyl group (3615 cm^{-1}) and the intramolecular hydrogen bonding (3207 cm^{-1}) are shown and better resolved at 1 mM concentration. However, it is not clear whether these bands originate from −OH···N intramolecular hydrogen bonding or from −OH···O intramolecular hydrogen bonding. Besides, the existence of a broad band around 3400 cm^{-1}, which is a similar frequency for −OH···O intermolecular hydrogen bonding, is also observed in the spectrum of 1 mM. Since the possibility of −OH···O intermolecular association is low in 1 mM concentration, this broad band might originate from another intramolecular association, such as −OH···O intramolecular hydrogen bonding. This complexity will be investigated in detail using the asymmetric dimers which have a simpler hydrogen bonding schemes. In addition, it is interesting that the band centered at 3559 cm^{-1}, which is independent of concentration, is observed. Although the assignment for this band cannot be precisely determined from these spectra, it is clear that this band originates from the intramolecular association. The nature of this band will be discussed later.

Features similar to the Methyl-dimer are shown in the FT-IR spectrum of Aniline-dimer in CCl_4 (Figure 5). However, the amount of intermolecular hydrogen bonding, which is represented by the intensity of the band centered at 3421 cm^{-1}, is relatively small compared to the spectrum of Methyl-dimer in 50 mM concentration. Instead, the band at 3549 cm^{-1}, which is suspected to be an intramolecular association, is significantly increased. This means that the large amount of OH groups, which formed intermolecular hydrogen bonding in the crystal state, became liberated in solution and turned into the intramolecular association. Again, a more detailed investigation for this intramolecular association will be done later in this paper by examining the FT-IR spectra for asymmetric dimers. One more interesting point is that the overall FT-IR spectrum of the BA-a polymer is similar to that of the Aniline-dimer spectrum in CCl_4, which is logical, taking into account that the present polybenzoxazines are thermoset polymers and are, therefore, amorphous. As a result, the FT-IR spectrum of the hydroxyl stretching region of Aniline-dimer in CCl_4, which is not restricted by a physically ordered structure, is suitable to simulate the BA-a polymer spectrum.

Asymmetric Dimers. Although the results from symmetric dimers can be used to hypothesize the hydrogen bonding structures of polybenzoxazines, they show complex hydrogen-bonded structures. As is shown in Schemes 2 and 7, when one benzoxazine ring is opened, only one Mannich bridge is formed, and thus, a polybenzoxazine has one hydroxyl group per one Mannich bridge. However, since the symmetric models have two hydroxyl groups for each Mannich bridge, one extra hydroxyl group makes the distinction between the −OH···O intramolecular hydrogen bonding and −OH···N intramolecular hydrogen bonding difficult. In addition, since half of the −OH groups in the dimers may be involved in intermolecular hydrogen bonding, the realistic contribution of hydroxyl group to intermolecular hydrogen bonding in polymers cannot be simulated accordingly. To eliminate these possibilities, asymmetric model dimers having only one −OH group in the structure were synthesized. As is shown in Schemes 3b and 3e, only two kinds of hydrogen bonding can be formed in these asymmetric dimers; one is −OH···O intermolecular hydrogen bonding, and the other is −OH···N intramolecular hydrogen bonding. Based on these asymmetric dimers, the actual contribution of each hydrogen-bonded species to the FT-IR spectrum can be examined.

From the FT-IR spectrum of the asymmetric Methyl-dimer (Figure 6), intramolecular hydrogen bonding is observed in the liquid phase. No intermolecular hydrogen bonding exists even in the liquid phase of asymmetric Methyl-dimer. Since the

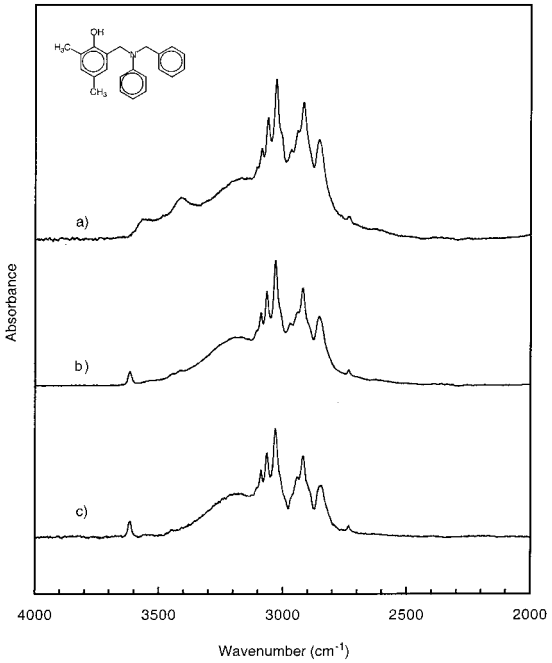

Figure 7. FT-IR spectra for asymmetric Aniline-dimer (a) in liquid phase, (b) in solution state in CCl_4 (50 mM), and (c) in solution state in CCl_4 (1 mM).

asymmetric dimer has only one hydroxyl group in the structure, if the stretching band for the −OH···O intermolecular hydrogen bonding is not shown, it can be concluded that only the intramolecular hydrogen bonding exists in the asymmetric Methyl-dimer. Furthermore, no evidence of free hydroxyl groups is observed even at 1 mM concentration. This strongly supports that −OH···N intramolecular hydrogen bonding in the Methyl-dimer is very stable and all hydroxyl groups in the asymmetric Methyl-dimer are participating in the −OH···N intramolecular hydrogen bonding.

On the other hand, a significant amount of intermolecular hydrogen bonding is found in the spectrum of asymmetric Aniline-dimer in the liquid phase (Figure 7a). This means that the hydroxyl groups in the asymmetric Aniline-dimer are competitively forming the −OH···N intramolecular hydrogen bonding or −OH···O intermolecular hydrogen bonding. Furthermore, as shown in Figure 7, parts b and c, the free hydroxyl stretching mode observed in the FT-IR spectrum of the asymmetric Aniline-dimer in CCl_4 suggests that a considerable amount of the hydroxyl groups, which formed the intermolecular hydrogen bonding in the liquid phase, are freed by the dilution.

From the evaluation of FT-IR spectra of the asymmetric dimers, the concentration-independent bands at 3113 cm^{-1} (for the asymmetric Methyl-dimer) and 3168 cm^{-1} (for the asymmetric Aniline-dimer) can be assigned to −OH···N intramolecular hydrogen bonding. The stretching frequency for this −OH···N intramolecular hydrogen bonding can be more clearly resolved in the spectra of 1 mM CCl_4 solution. This assignment agrees well with the typical chelated hydrogen bonds in Mannich bridges reported by several authors.[7,16] It can also be assigned the band at 3417 cm^{-1} to the −OH···O intermolecular hydrogen bonding because this band in the asymmetric Aniline-dimer in the liquid phase shows concentration dependency. However, in the case of symmetric dimers, a broad band still exists around 3400 cm^{-1} even at the dilute concentration of 1 mM. Hence, it implies the possibility of overlapped intermolecular and intramolecular hydrogen-bonded OH bands near 3400 cm^{-1} in symmetric dimers.

SCHEME 4: Proton-Transfer Equilibrium in Mannich Bases

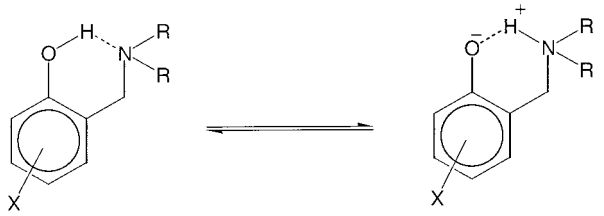

In addition, it is interesting that the stretching band for protonated nitrogen exists, which is demonstrated by the broad tail around 2700 cm^{-1} to 2400 cm^{-1} in both asymmetric dimers. The existence of proton-transfer equilibrium (OH···N ↔ O^-···H^+N) has been reported for the hydrogen bonding system in Mannich base which is a direct analogue of phenol−amine complex (Scheme 4).[16−20] Especially, Rospenk and Zeegers-Huyskens[18] reported that the stretching band for −O^-···H^+N intramolecular hydrogen bonding is observed between 2800 and 2700 cm^{-1} using 2-(*N*,*N*-dodecylaminomethyl)-3,6-dichloro-4-nitrophenol and its −OD deuterated analogue. From the curve-fitting results of the spectra in 1 mM solution shown in Figure 8, it is obvious that the existence of protonated nitrogen is demonstrated by the bands at 2750 cm^{-1} (asymmetric Methyl-dimer) and at 2830 cm^{-1} (asymmetric Aniline-dimer).

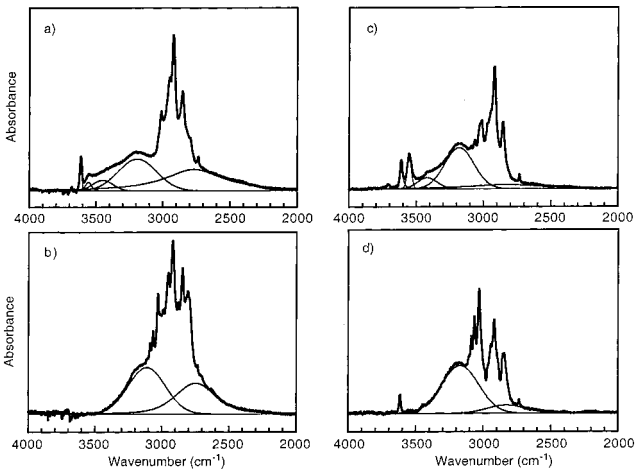

Figure 8. Curve fitting for FT-IR spectra of symmetric dimers in CCl_4 solution (1 mM); (a) Methyl-dimer and (b) Aniline-dimer.

From the comparison of the curve-resolved band for the protonated nitrogen, it is noticeable that the intensity of the band at 2750 cm^{-1} for the asymmetric Methyl-dimer is much stronger than that for the asymmetric Aniline-dimer. This means that the proton-transfer equilibrium (OH···N ↔ O^-···H^+N) in the asymmetric Aniline-dimer is shifted to the left-hand side, and thus, the polarizability of a proton in Mannich base is affected by the amine functional group. Consequently, this difference in the proton-transfer equilibrium can also be used for explaning why the asymmetric Aniline-dimer shows the bands for free hydroxyl group and intermolecular hydrogen bonding while the asymmetric Methyl-dimer has only intramolecular hydrogen bonding even in a very diluted concentration.

−OH···π Hydrogen Bonding. As mentioned in the symmetric dimers section, although the shoulder band at 3559 cm^{-1} in the Methyl-dimer and strong band at 3547 cm^{-1} in the Aniline-dimer have the nature of intramolecular association because those are not dependent on concentration, the origin of this stretching band cannot be precisely determined. The

SCHEME 5: Hydrogen Bonding in Asymmetric Aniline-dimer. (A) −OH···N Intramolecular Hydrogen Bonding, (B) −OH···π Intramolecular Hydrogen Bonding, (C) −OH···π Intermolecular Hydrogen, and (D) −OH···O Intermolecular Hydrogen Bonding

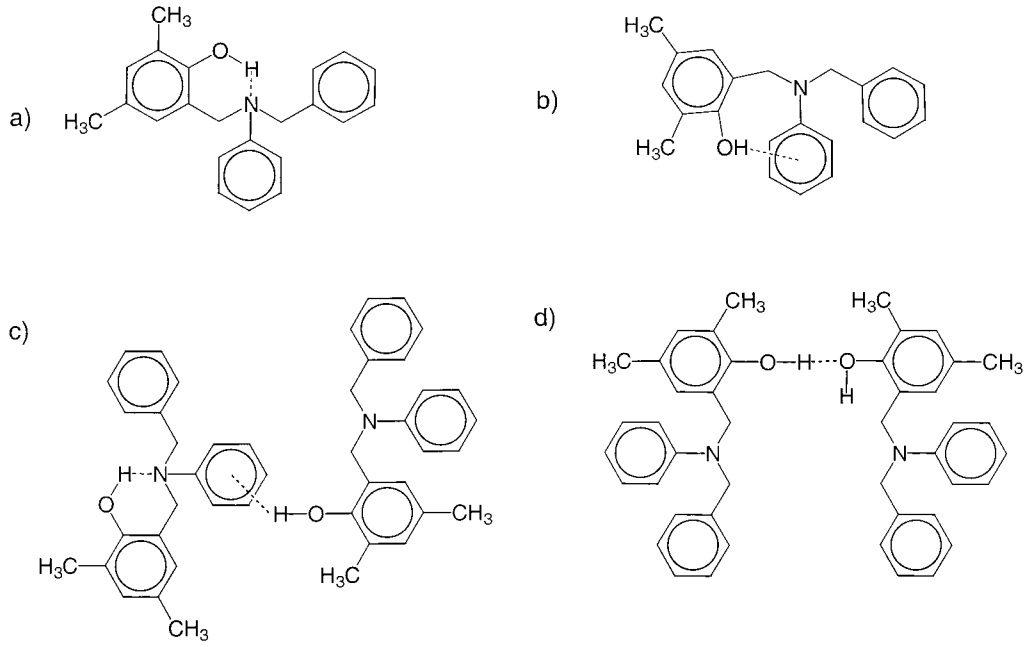

assignment for this band in the Methyl-dimer was attempted by Dunkers et al.,[7] but they could not explain this band clearly. However, using simple hydrogen bonding structure of asymmetric dimers, this band can be investigated in more detail. Despite the simple hydrogen bonding scheme in the asymmetric Aniline-dimer, the FT-IR spectrum of the asymmetric Aniline-dimer in the liquid phase shows that there is a new band other than −OH···N intramolecular or −OH···O intermolecular hydrogen bonding (Figure 7a). According to Pimentel and McClellan,[21] hydrogen bonding exists between the proton of acids and aromatics because aromatics act as good electron donors. And, according to Cairns and Eglinton,[14] it has been reported that −OH···π intramolecular hydrogen bonding is observed at 3516 cm^{-1} in the infrared spectrum of well-designed novolac dimers. They also concluded that this −OH···π intramolecular hydrogen bonding is highly affected by the conformation of molecules.

A similar explanation can be applied to the benzoxazine model dimers. In the asymmetric Aniline-dimer, the hydroxyl groups which are not intramolecularly associated can form either −OH···O intermolecular hydrogen bonding (Scheme 5d) or −OH···π hydrogen bonding (Scheme 5b and 5c) as long as the conformational proximity is allowed. However, since most of the hydroxyl groups in the asymmetric Methyl-dimer are involved in −OH···N intramolecular hydrogen bonding, there are no available hydroxyl groups to form −OH···π hydrogen bonding.

More compelling evidence that −OH···π intramolecular hydrogen bonding exists can be found in the Aniline-dimer. That is, since one extra hydroxyl group is available in the symmetric dimers (Scheme 6), the formation of −OH···π intramolecular hydrogen bonding is possible as well as relatively free hydroxyl group. Also, the existence of aniline in the Aniline-dimer structure makes the −OH···π intramolecular hydrogen bonding conformation more favorable. The observation of a concentration-independent band at 3549 cm^{-1} in Figure 5 supports this bond formation.

Polybenzoxazines and Hydrogen Bonding. As was mentioned above, the hydrogen-bonded network structure of the

SCHEME 6: Hydrogen Bonding in Aniline-dimer. (A) −OH···N Intramolecular Hydrogen Bonding, (B) −OH···π Intramolecular Hydrogen Bonding, and (C) −OH···O Intermolecular Hydrogen Bonding

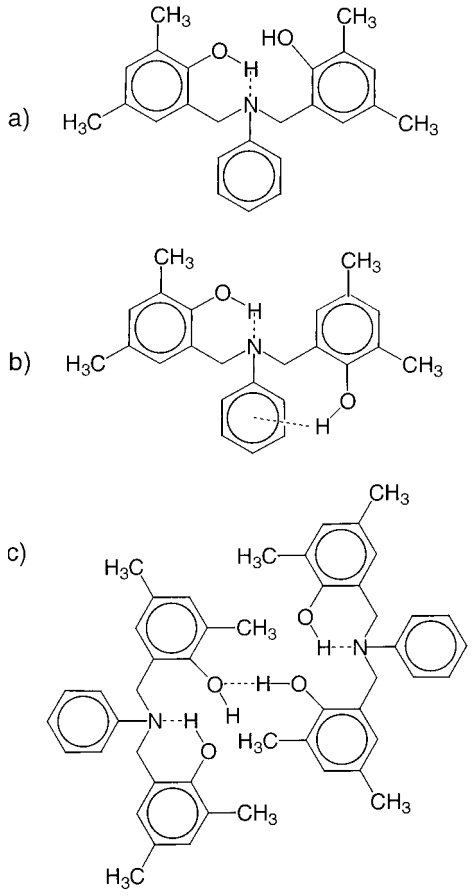

BA-m and BA-a polymers has been explained by the results obtained from the experiments using aliphatic amine model dimers—mainly the Methyl-dimer. However, from this system-

SCHEME 7: Proposed Hydrogen-Bonded Network Structure for Two Typical Polybenzoxazines

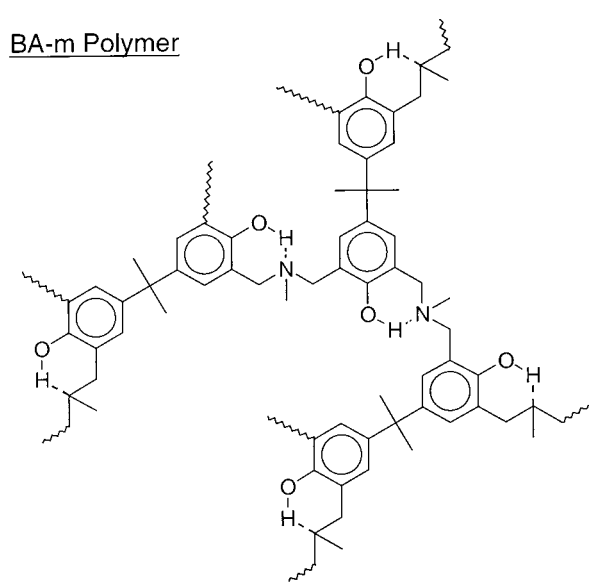

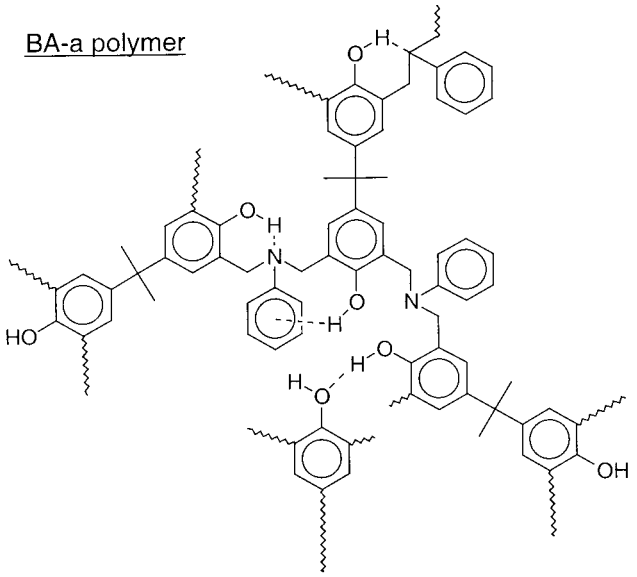

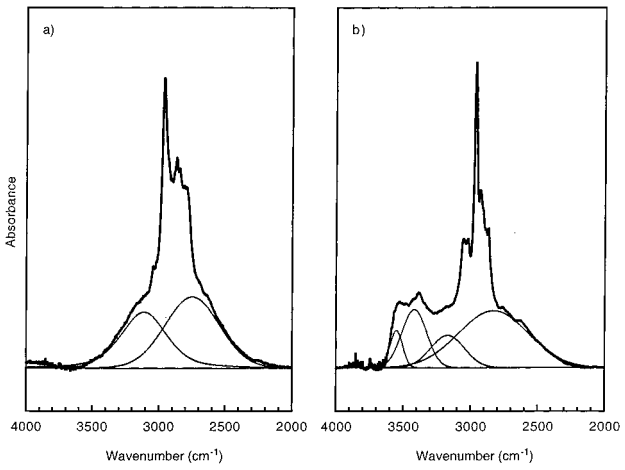

Figure 9. Curve fitting for FT-IR spectra of polybenzoxazines; (a) BA-m polymer and (b) BA-a polymer.

TABLE 1: Vibrational Assignments for Hydrogen Bonding Species in Model Dimers and Polybenzoxazines

	state	ν_{Free}[a]	$\nu_{OH-\pi}$[b]	ν_{OH-O}[c]	ν_{OH-N}[d]	ν_{O-HN}[e]
Methyl-dimer	crystal		3559	3401	3207	2768
	50 mM	3615	3559	3401	3207	2768
	1 mM	3615	3559	*3476	3207	2768
Aniline-dimer	crystal		3549	3421	3219	2831
	50 mM	3614	3549	3421	3217	2831
	1 mM	3614	3549	*3421	3181	2831
asym.	liquid				3113	2750
Methyl-dimer	50 mM				3113	2750
	1 mM				3113	2750
asym.	liquid		3549	3417	3168	2830
Aniline-dimer	50 mM	3617		3417	3168	2830
	1 mM	3617			3170	2830
BA-m	polymer				3112	2749
BA-a	polymer		3550	3417	3171	2830

[a] Wavenumber (cm^{-1}) of relatively free hydroxyl group. [b] Wavenumber (cm^{-1}) of $-OH\cdots\pi$ intramolecular hydrogen bonding. [c] Wavenumber (cm^{-1}) of $-OH\cdots O$ intermolecular hydrogen bonding. (* assigned to $-OH\cdots O$ intramolecular hydrogen boning). [d] Wavenumber (cm^{-1}) of $-OH\cdots N$ intramolecular hydrogen bonding. [e] Wavenumber (cm^{-1}) of $-O^{-}\cdots H^{+}N$ intramolecular hydrogen bonding.

atic study for hydrogen bonding in the model dimers, a more clear explanation for the relationship between the properties of polybenzoxazines and the network structures can be given. To determine the fraction of each hydrogen bonding species in polybenzoxazines, the FT-IR spectra for polymers are curve-resolved by using the corresponding frequencies of each hydrogen bonding species, as illustrated in Figure 9 and the results are summarized in Table 1. Although the differences in the specific absorptivities for each hydrogen bonding species must be taken into account, a qualitative assessment for the distribution of hydrogen bonding species can be made by the comparison of each of the fraction. Therefore, the relationship between the properties of the polymer and the distribution of hydrogen bonding species will be discussed in this section.

While the network structure of the BA-m polymer mainly consists of $-OH\cdots N$ and $-O^{-}\cdots H^{+}N$ intramolecular hydrogen bonding, the BA-a polymer has a relatively small amount of intramolecular hydrogen bonding. Instead, the large portion of hydroxyl groups in the BA-a polymer forms either weak $-OH\cdots\pi$ intramolecular hydrogen bonding or $-OH\cdots O$ intermolecular hydrogen bonding (Scheme 7). Consequently, this supports the previous hypothesis that the BA-m polymer chains are more highly curled due to intramolecular hydrogen bonding.[3] Although polybenzoxazines are chemically cross-linked by the ring-opening reaction of the benzoxazine rings, the cross-linking density is too low to explain the very high modulus of polybenzoxazines. Therefore, it is believed that the physical interaction of polymer chains due to hydrogen bonding plays an important role in fostering the excellent properties of polybenzoxazines. In addition, the difference in the distribution of hydrogen bonding in the polymer presents more supporting evidence for the higher volumetric expansion value of the BA-m polymer (Table 2), by the molecular curling due to the preferential $-OH\cdots N$ intramolecular hydrogen bonding. Since the BA-m polymer chains are highly curled, rather than extended, due to the $-OH\cdots N$ intramolecular hydrogen bonding, it is difficult to tightly pack the BA-m polymer chains, thus leading to volumetric expansion. On the other hand, a large amount of the hydroxyl groups in the BA-a polymer are involved in intermolecular hydrogen bonding or in the form of relatively weak intramolecular hydrogen bonds. As a result, since the intermolecular hydrogen bonding has a significant effect on the packing of polymer chains, the BA-a polymer chain may have a chance to be more extended during the ring opening polymerization and, therefore, show low volumetric expansion.

SCHEME 8: Penetration of Water or Acetic Acid Molecules

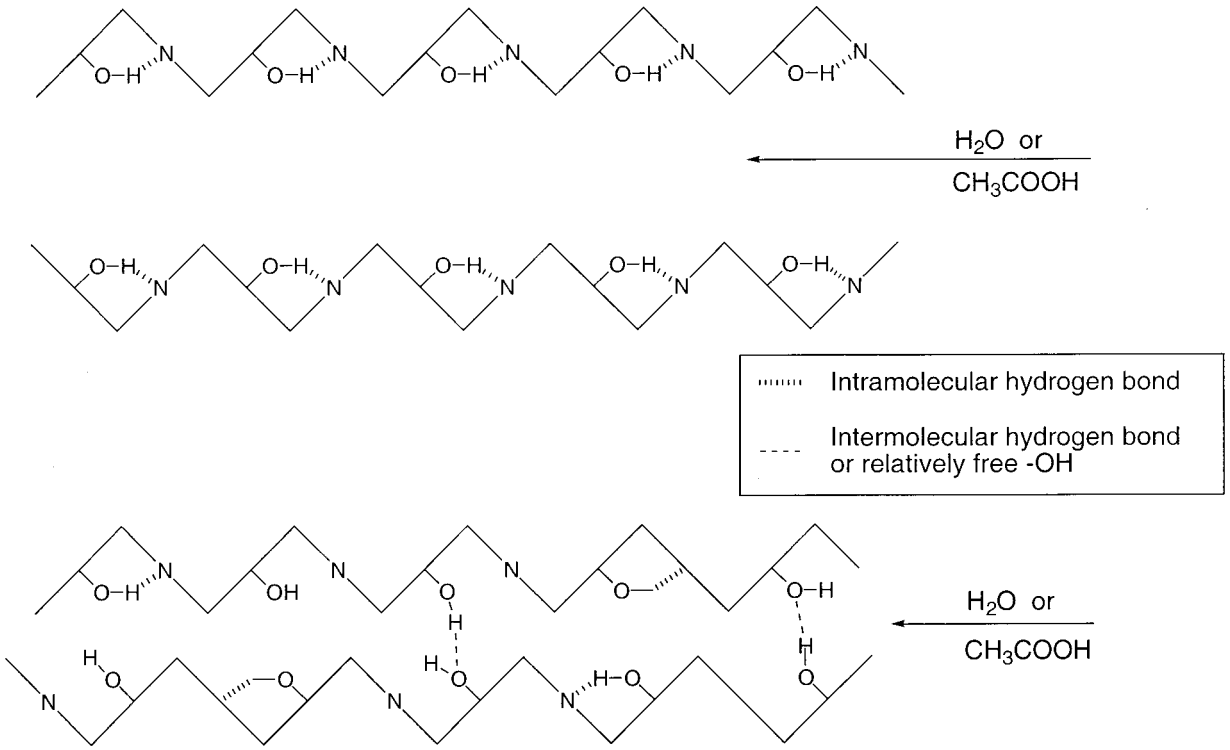

TABLE 2: Comparison of Physical Properties for the BA-a and BA-m Polymer

	BA-m polymer	BA-a polymer
vol. expansion(%)[3]	+3.2%	−0.4%
water absorption[1]		
diffusion coef.	3.6×10^9 cm^2/s	0.5×10^9 cm^2/s
saturation	1.3%	1.9%
cross-link density[1]	$<1.1 \times 10^3$mol/cm^3	1.1×10^3mol/cm^3
resistance to		
carboxylic acid[4]	poor	excellent
UV light[5]	poor	excellent

In addition, since the BA-a polymer has additional reaction sites on the aniline functional group in Mannich bridge,[22,23] it is obvious that the BA-a polymer is more chemically cross-linked and has tighter packing than the BA-m polymer.

The other interesting behavior is the low water absorption of these polybenzoxazines having large numbers of hydroxyl groups. Despite the belief that the BA-m polymer has a bulkier structure than the BA-a polymer, the percentage of weight gain at saturation for the BA-m polymer is smaller than that of the BA-a polymer, even though the BA-m polymer has a larger diffusion coefficient. The larger diffusion coefficient of the BA-m polymer is responsible for the bulkier network structure, which results in a greater free volume for water to penetrate. However, the fact that the BA-m polymer has smaller water uptake at saturation is somewhat conflicted at a first glance with the result of higher diffusion coefficient for the BA-m polymer. Although the larger free volume provides greater diffusion coefficient, the environment within the free space is more hydrophobic in the BA-m polymer, as the majority of the hydroxyl groups form intramolecular hydrogen bonding with the nitrogen atoms, thus leading to an expected lower water uptake (Scheme 8). As discussed previously in the model dimer study, the −OH···N intramolecular hydrogen bonding in the BA-m polymer is stable, and so is difficult to be disturbed by water molecules. However, the hydroxyl groups in the BA-a polymer such as in the relatively free hydroxyl group and −OH···π intramolecular hydrogen bonding might be involved in the interaction with water molecules because those hydrogen bondings can be easily interrupted which, in turn, lead to the higher saturation value.

Additionally, this can be supported by the explanation for the excellent chemical stability of the BA-a polymer in carboxylic acid that was proposed in a previous paper.[4] That is, carboxylic acid molecules can penetrate into the BA-m polymer more easily due to the bulkier network structure, as well as the affinity of carboxylic acid for the Mannich bridge, resulting in macroscopic stress cracking by solvents. On the other hand, since the BA-a polymer may have a tighter network structure, the relatively large carboxylic acid molecules have difficulty penetrating into the polymer structure.

Conclusions

The hydrogen bonding architectures in polybenzoxazines have been investigated utilizing the FT-IR spectra of model dimers and polymers. From the comparison of the FT-IR spectra of the polybenzoxazines and model dimers, it has been shown that the simpler structure of the asymmetric dimers well simulates the hydrogen-bonded network structure between polymer chains while the structure of symmetric dimers reflects the hydrogen bonding scheme related to the end-groups of polymer chains. Furthermore, it has been shown that the BA-m polymer consists mainly of −OH···N and $-O^-\cdots H^+N$ intramolecular hydrogen bonding, while the BA-a polymer has a large amount of intermolecular hydrogen bonding and relatively weak intramolecular hydrogen bonding in the polymer network structure. From the results of the model dimer study, it has been found that the amine functional group in the Mannich bridges is greatly responsible in influencing the distribution of the hydrogen bonding species. Possible hydrogen bonding network structures for the BA-m and BA-a polymers were proposed. Consequently,

generalized explanations for the relationships between the hydrogen-bonded network structure and the excellent properties of polybenzoxazines, such as the volumetric expansion, water absorption, and resistance to carboxylic acid have also been discussed.

References and Notes

(1) Ishida, H.; Allen, D. J. *J. Polym. Sci., Polym. Phys.* **1996**, *34*, 1019.
(2) Shen, S. B.; Ishida, H. *Polym. Comput.* **1996**, *17*, 710.
(3) Ishida, H.; Low, H. Y. *Macromolecules* **1997**, *30*, 1099.
(4) Kim, H. D.; Ishida, H. *J. Appl. Polym. Sci.*, accepted.
(5) Macko, J.; Ishida, H. *J. Polym. Sci., Polym. Phys.* **2000**, *38*, 2687.
(6) Ishida, H.; Rodriguez, Y. *Polymer* **1995**, *36*, 3151.
(7) Dunkers, J. P.; Zarate, A.; Ishida, H. *J. Phys. Chem.* **1996**, *100*, 13514.
(8) Wirasate, S.; Dhumrongvaraporn, S.; Allen, D. J.; Ishida, H. *J. Appl. Polym. Sci.* **1998**, *70*, 1299.
(9) Ning, X.; Ishida, H. *J. Polym. Sci., Polym. Chem. Ed.* **1994**, *32*, 1121.
(10) Ishida, H. U.S. Pat. 5,543,516, Aug. 6, 1996.
(11) Dunkers, J.; Ishida, H. *Spectrochim. Acta* **1995**, *51A* (5), 855.
(12) Goss, F. R.; Ingold, C. K.; Wilson, I. S. *J. Chem. Soc.* **1926**, 2440.
(13) Brycki, B.; Maciejewska, H.; Brzezinski, B.; Zundel, G. *J. Mol. Struct.* **1991**, *246*, 61.
(14) Cairns, T.; Eglinton, G. *J. Chem. Soc.* **1965**, 5906.
(15) Kovac, S.; Eglinton, G. *Tetrahedron* **1969**, *25*, 3599.
(16) Sucharda-Sobczyk, A.; Sobczyk, L. *J. Chem. Res.* **1985**, 208.
(17) Albrecht, G.; Zundel, G. *J. Chem. Soc., Faraday Trans. 1* **1984**, *80*, 553.
(18) Rospenk, M.; Zeegers-Huyskens, T. *J. Phys. Chem.* **1987**, *91*, 3974.
(19) Koll, A.; Rospenk, M.; Sobczyk, L. *J. Chem. Soc., Faraday Trans. 1* **1981**, *77*, 2309.
(20) Rospenk, M.; Sobczyk, L. *Magn. Reson. Chem.* **1989**, *27*, 445.
(21) Pimentel, G. C.; McClellan, A. L. *The Hydrogen Bond*; W. H. Freeman and Company: London, 1960; pp 202−203.
(22) Low, H. Y.; Ishida, H. *Polymer* **1999**, *40*, 4365.
(23) Ishida, H.; Sanders, D. P. *Macromolecules*, accepted.